DC-offset Estimation of Multiple CW Micro Doppler Radar

Dong Kyoo Kim
Hyper-connected Research Lab
Electronics and Telecommunications Research Institute
line 4: Daejeon, South Korea
kdk3606@etri.re.kr

You Jin Kim
Hyper-connected Research Lab
Electronics and Telecommunications Research Institute
line 4: Daejeon, South Korea
youjin@etri.re.kr

***Abstract*— Dc-offset estimation of quadrature continuous-wave (CW) radar has been studied for years. Studies have shown that the estimation error increases when target movement with respect to the radar is small. This paper presents a method that uses multiple simultaneous CW frequencies for the dc-offset estimation, which makes the dc-offset estimation easy in contrast to the conventional quadrature CW radar. A dc-offset estimation method using the multiple CW frequencies is presented to demonstrate that the multiple CW frequencies provide sufficient information for the dc-offset estimation.**

***Keywords*— Center estimation, Micro Doppler radar, Dc-offset.**

I. INTRODUCTION

Respiration, heartbeat rate, and heart rate variability using radars are the most interest to researchers. Respiration sensing have been studied in [1][2][3], and related products start to be released. Heartbeat signals have been also intensively studied [4][5]. For both cases, CW radars were used to detect human chest movements. CW radar is a simple transceiver with a single oscillator, in which the receiver coherently mixes the transmitted signal by branching the transmitted signal. Quadrature CW radar has quadrature receiver architecture [6], in which the received signal is mixed by two orthogonal oscillating signals, as shown in Fig. 1. The resultant mixed signals are called I and Q signals. Target movement changes the phase of the quadrature CW radar, which can be obtained by linear or non-linear demodulation [4]. Linear demodulation is the small angle approximation when the movement is much smaller than the oscillator wave length; for example, the movement is smaller than $\lambda/4\pi$ in [4]. Non-linear demodulation is also called arctangent demodulation because the phase information is obtained by $tan^{-1}(Q/I)$. Arctangent demodulation can be used to precisely calculate the target movement if it is smaller than λ. The problems of non-linear demodulation are I/Q imbalance and dc-offset [4],[7],[8],[9]. I/Q imbalance introduces errors in the measurement of the phase information [6]. The I/Q imbalance measurement can be conducted by using a phase shifter [10] or an automatic milling machine [11], which is used for artificially moving the target. The imbalance is eliminated by using Gram-Schmidt procedure [10]. In [9][11][12], the imbalance was calculated and compensated by using ellipse fitting algorithms. The dc-offset is known to be caused by reflections from stationary objects and hardware imperfections [4]. The dc-offset floats when the objects move. The dc-offset appears as bias in the I and Q signals, where each bias value is different. The dc-offset affects the critical performance of the movement estimation [13]. In the complex plane of I and Q, the I and Q signals due to the target movement are described as an arc, and the dc-offset is the center of the arc [8]. Several center estimation methods have been studied for the dc-offset estimation [5][8][9][14][15]. In [8], a heuristic method was presented, and in [5], the heuristic method and geometric fitting method was compared. In [5], center estimation methods suitable for real-time implementations were analyzed. High performance techniques using ℓ_1-minimization have also been proposed for geometric distance minimization [9] and for algebraic distance minimization [14][15]. Linear programming is known for its high computational complexity, and its real-time implementation is still under research. In the literature, short arc lengths have always been found to affect the performance of their center estimation methods.

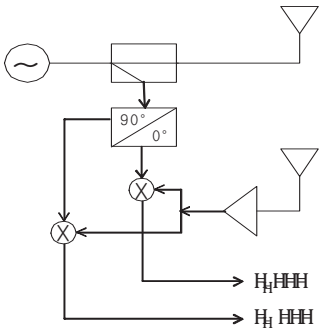

Fig. 1. Quadrature CW radar architecture

This paper first describes the center estimation methods for the quadrature CW radar, and its center estimation methods are presented in Section II. In Sections III and IV, a multiple CW quadrature radar and its center estimation methods are presented. The multiple CW quadrature radar is a means of handling the short arc length problem. It provides an extended arc while the target movement conditions are the same. Then, a dc-offset estimation method is presented. Simulation results are provided in Section V to demonstrate that the multiple CW quadrature radar can efficiently estimate the center of an arc, whereas the quadrature CW radar cannot be estimated. A summary of this paper is provided in Section VI.

II. QUADRATURE CW RADAR

The quadrature CW radar shown in Fig. 1 transmits a stable wave energy with frequency f, which is expressed as

$$s(t) = A_{tx}\cos(2\pi ft + \phi(t)), \quad (1)$$

ISBN 978-90-827970-1-5

where ϕ is the random phase noise of the transmitter. The transmitted signal is reflected from objects within the radar radiation area. In this paper, it is assumed that the reflection comes from a human chest. Thus, the received signal shown in Fig. 1 is the sum of the dominant chest reflection signal and other object reflections. We can express the output signal of the receiver as

$$r(t) = A_0 \cos\left(4\pi\lambda^{-1}d + 4\pi\lambda^{-1}x(t) + \varphi_0 + \Delta\phi(t)\right) + jA_0A_e \sin(4\pi\lambda^{-1}d + 4\pi\lambda^{-1}x(t) + \varphi_0 + \Delta\phi(t) + \phi_e) + +DC_I(t) + jDC_Q(t) + w(t) \quad , \quad (2)$$

where is A_0 the baseband amplitude, λ is the wavelength of the transmitter frequency f, d is the nominal distance between the radar and the main target object (human chest in this paper), $x(t)$ is the small displacement of the main target ($|x(t)| < \lambda$), φ_0 is the initial phase offset, $\Delta\phi$ is the phase noise difference between the phase noise and the time-delayed phase noise, and $w(t)$ is white Gaussian noise. A_e and ϕ_e are amplitude and phase imbalance of the in- and quadrature-phase channels, which is caused by circuit imperfection factors. The imbalance can be measured and eliminated by the Gram–Schmidt procedure [7]

$$\begin{bmatrix} I(t) \\ Q(t) \end{bmatrix} = \begin{bmatrix} 1 & 0 \\ -\tan\phi_e & \frac{1}{A_e\cos\phi_e} \end{bmatrix} \begin{bmatrix} r_I(t) \\ r_Q(t) \end{bmatrix}. \quad (3)$$

DC_I and DC_Q in (2) are the dc-offsets of the in- and quadrature-phase channels. The dc-offset is known to be caused by reflections from stationary objects and hardware imperfections [4]. The dc-offset induced by hardware imperfection can be easily eliminated by the pre-measurement method; however, the dc-offset still remains and varies as the position of the target and other objects changes. When the target objects are stationary, DC_I and DC_Q in (2) are constant; otherwise, they change over time. If the dc-offset changes slowly, it can be said that the dc-offset is constant for some time interval, i.e., quasi-stationary. Then, (2) can be written as

$$r_i(t) = A_{0,i}\cos\left(4\pi\lambda^{-1}d_i + 4\pi\lambda^{-1}x(t) + \varphi_0 + \Delta\phi(t)\right) + jA_{0,i}\sin\left(4\pi\lambda^{-1}d_i + 4\pi\lambda^{-1}x(t) + \varphi_0 + \Delta\phi(t)\right) + DC_{I,i} + jDC_{Q,i} + w(t) \quad , \quad (4)$$

where $0 \le t < T, i = 0,1,2,\ldots$, $r_i(t) = r(t - iT)$, and T is the quasi-stationary time interval. This condition is quite reasonable in the case of the experiment scenarios that have been considered in heartbeat measurement radar research.

We assume that the phase noise is small $\Delta\phi(t) \approx 0$ and the received signal is sufficiently large against $w(t)$. Then, (4) can be simply written as

$$r_i(t) \simeq A_{0,i}\cos(4\pi\lambda^{-1}d_i + 4\pi\lambda^{-1}x(t) + \varphi_0) + jA_{0,i}\sin(4\pi\lambda^{-1}d_i + 4\pi\lambda^{-1}x(t) + \varphi_0) + DC_{I,i} + jDC_{Q,i} \quad , \quad (5)$$

which is depicted as a complex plot in Fig. 2. As shown in Fig. 2, d gives no information in the complex plot because d is shown as multiple rotations tracing on the dotted circle. To simplify the explanation, we eliminate the d term in this section as

$$r_i(t) \simeq A_{0,i}\cos(4\pi\lambda^{-1}x(t) + \varphi_0) + jA_{0,i}\sin(4\pi\lambda^{-1}x(t) + \varphi_0) + DC_{I,i} + jDC_{Q,i} \quad . \quad (6)$$

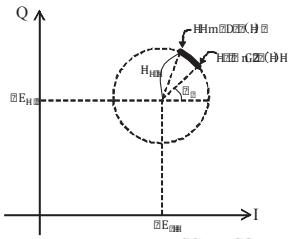

Fig. 2. Complex plot representation of $r_i(t)$: $r_i(t)$ due to the displacement $x(t)$ is located in the thick arc.

III. Multiple CW Quadrature Radar and its DC-offset Estimation

A multi-frequency quadrature radar is shown in Fig. 3, in which the frequency f of the transmitter is variable. This architecture has been used for frequency-modulation CW (FMCW) radar, step-frequency CW (SFCW) radar, and other research areas in many studies [16][17]. The output of the receiver shown in Fig. 3(a) can be written as

$$r_i(t, f_m) = A_{0,i}(m)\cos(4\pi c^{-1}f_m p(t) + \varphi_0) + jA_{0,i}(m)\sin(4\pi c^{-1}f_m p(t) + \varphi_0) + DC_{I,i} + jDC_{Q,i} \quad , \quad (7)$$

where the d_i term in (4) is reconsidered as $p(t) = d_i + x(t)$, and the discrete frequency value is considered such as SFCW radar; $m = 0, \ldots, M-1$; (7) is equivalent to (6) where $c = f\lambda$, and $c = 3 \times 10^8$ (m/s) is the speed of light. If the frequency sweep time is sufficiently fast, the displacement $x(t)$ is constant for the sweep time. Thus, (7) can be written as

$$r_i(n, f_m) = A_{0,i}(m)\cos(4\pi c^{-1}f_m p(n) + \varphi_0) + jA_{0,i}(m)\sin(4\pi c^{-1}f_m p(n) + \varphi_0) + DC_{I,i} + jDC_{Q,i} \quad , \quad (8)$$

where $p_i(n) = d_i + x(n)$. (8) is the representation of the multi-frequency quadrature radar. The set of frequencies, i.e., $\mathbf{F} = \{f_0, f_1, \ldots, f_{M-1}\} = \{f_c, f_c + \Delta f, \ldots, f_c + (M-1)\cdot\Delta f\}$ lies within a frequency band, where f_c is the carrier frequency of the band, and Δf is the adjacent frequency difference. The popular radar bands are 2.4 GHz, 10 GHz, 24 GHz, etc. In these bands, the received signal power values do not vary considerably over $\mathbf{F}$. For example, Fig. 4(a) shows the received signal power of $f_c = 24$ GHz and $\Delta f = 30$ MHz, and Fig.

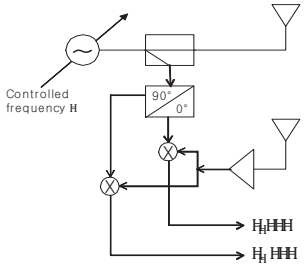

Fig. 3. Multiple CW quadrature radar architecture

4(b) shows the received signal power of $f_c = 2.4\ GHz$ and $\Delta f = 3\ MHz$, where the transmitted signal power is assumed to be $1\ mW$ and the path loss of the transmitted signal is considered as the free-space path loss equation [18] as follows

$$FSPL(p(n), f_m) = 20log_{10}(p(n)f_m) - 147.55, \quad (9)$$

where $p(n)$ is set to 1 m. In the figures, the variance of the received signal powers is less than 0.1 dB. In this case, we assume that $A_{0,t}(m)$ is independent from m, so that (8) can be written as

$$q_t(n, f_m) = A_{0,t}exp[j4\pi c^{-1} f_m p(n) + \varphi_0] + (DC_{I,t} + jDC_{Q,t})$$

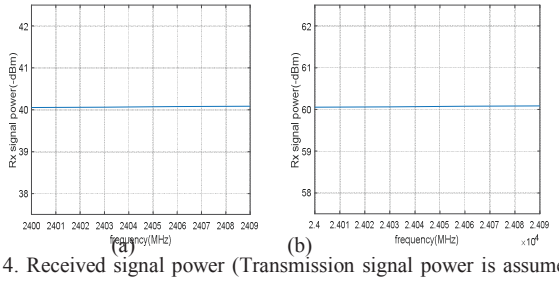

(a) (b)

Fig. 4. Received signal power (Transmission signal power is assumed to 1mW): (a) 24 *GHz* band and (b) 2.4 *GHz* band

. (10)

By considering white Gaussian noise, we write (10) with the noise $w(t)$ as

$$y_t(n, f_m) = q_t(n, f_m) + w(t), \quad (11)$$

We use three methods to estimate the center of (11) for the multi-frequency quadrature radar: the circumcenter method [19].

The circumcenter calculation method is as follows, where $M = 3$ is assumed. Three points are selected as $S = [y_t(n, f_0) \quad y_t(n, f_1) \quad y_t(n, f_2)]$. Then, the area of S, ΔS, is calculated. If $\Delta S > \epsilon$, the circumcenter can be calculated as

$$(\widehat{DC}_I, \widehat{DC}_Q) = \frac{\alpha S_1 + \beta S_2 + \gamma S_3}{\alpha + \beta + \gamma}, \quad (12)$$

where ϵ is a small value, e.g., 10^{-9}, $\alpha = a(b + c - a)$, $\beta = b(a + c - b)$, $\gamma = c(a + b - c)$, $a = |S_2 - S_3|$, $b = |S_1 - S_3|$, and $c = |S_1 - S_2|$. If $\Delta S < \epsilon$, another S should be taken for other n until $\Delta S > \epsilon$. If there is no S that satisfies $\Delta S > \epsilon$, the method fails. If Δf is carefully designed considering f_c, d, and Δx, the method would not fail. This method is summarized in Fig. 5.

The circumcenter method requires arc data having a largely distributed angle before the algorithm starts. The multi-frequency quadrature radar is adequate for acquiring such largely distributed arc data in a short time. For the quadrature CW radar, it is difficult to acquire such large arc data, and a longer time is required to obtain the arc dataset. For the quadrature CW radar, iterative geometric fitting method is advantageous [5], where the geometric fitting requires a quite accurate initial value and expensive iterations that may slow down the overall data processing.

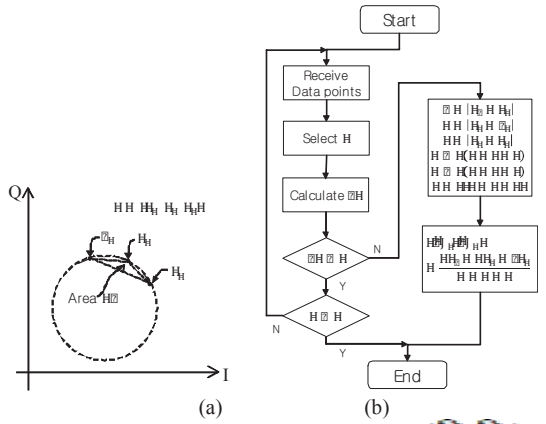

(a) (b)

Fig. 5. Circumcenter method: (a) If area $\Delta S > \epsilon$, the $(\widehat{DC}_I, \widehat{DC}_Q)$ is the circumcenter of the triangle S. (b) Flowchart

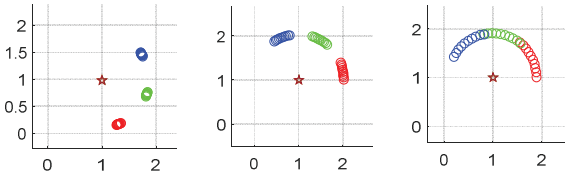

(a) (b) (c)

Fig. 6. Multiple arcs for different frequency bands. Arc center is commonly set to (1,1): (a) $f_c = 2.4\ GHz$ (b) $f_c = 10\ GHz$, and (c) $f_c = 24\ GHz$

IV. Simulation Results

It is assumed that the offsets of I and Q are neglected, which is rejected by the procedure described in Section II. Noise $w(t)$ on I and Q is considered as a 2D Gaussian distribution with zero mean. The noise variance is expressed as signal-to-noise ratio (SNR). The simulated target is at a distance of 1 m and periodically moves at Δx intervals. The movement modulates the phase of I and Q signals in the receiver, as in (11), and it is expressed as an arc on a circle in a complex plot. In the first simulation, it is shown how f_c affects the accuracy of the center estimation. Δx is set to 1 mm, and the data points are uniformly distributed within Δx. Δf is set to $20\ MHz$ and $M = 3$. SNR is set to 40 dB so that the arc shape can be clearly identified. Fig. 6 shows four complex plots for $f_c = 2.4\ GHz, 10\ GHz,$ and $24\ GHz$, in which the real center of the arcs is (1,1). Each complex plot has three arcs for three f_ms, and the star markers indicate the estimated dc-offset of the circumcenter estimation methods. Individual arc possession over a full circle is represented as a percentage. For a specific m, the arc possessions of the four f_c are 0.13%, 0.8%, 3.3%, and 8%, respectively. The advantage of the multi-frequency quadrature radar over the quadrature CW radar is that the arc possession can be extended, although the extension is discontinuous. The multi-frequency arc possessions are extended to 27.5%, 31.5%, 46.7%, and 42.7%. The arc possession directly affects the center estimation performance. The center estimation performance in our simulations is expressed as the normalized error:

ISBN 978-90-827970-1-5 © EURASIP 2018

$$Error = \frac{\|(DC_I, DC_Q) - (\widehat{DC}_I, \widehat{DC}_Q)\|}{R} \times 100 \ (\%), \quad (13)$$

where R is the radius of the true full circle. This expression is useful to predict the error propagation effect on the displacement estimation, for which the non-linear relationship is described in [13]. Fig. 7 shows the center estimation performance of the multi-frequency and the quadrature CW radar by using the previously mentioned parameters, in which the circumcenter method is used for the estimation. Fig. 7 shows that the discretely extended arc possession increases the center estimation performance. The quadrature CW radar with a small arc possession under 10% shows considerable performance deterioration. However, the multi-frequency quadrature radar increases the performance as the arc possession increases. The amplitude variance is small, such that the center estimation error is below 3%, which guarantees very small displacement estimation deviation error, according to Fig. 3 in [13]. And this also shows that the assumption in (13) is correct.

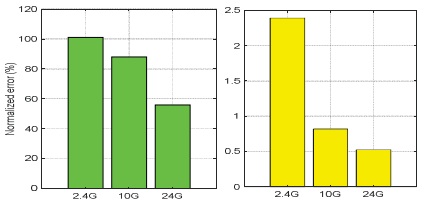

Fig. 7. Performance of the center estimation methods for different frequency bands: (a) quadrature CW radar and (b) multiple CW quadrature radar

We consider how random noise in the I and Q signals affects the center estimation performance. For $f_c = 24\ MHz$, the performance comparisons with SNR variations from 20 dB to 50 dB are shown in Fig. 8, where the estimation method is the circumcenter method. In this figure, at least $SNR = 21\ dB$ is required in order to obtain a center estimation error of less than 10%. Respiration and heartbeat signals are not uniformly distributed within Δx. Many studies [1][4][20] have modeled the physiological signal as simple single tones with their proper frequencies according to respiration and heartbeat. This single tone representation does not accurately describe the physiological signal, but more accurate models have been proposed in [21],[22]. In [21], the heartbeat signal was modeled as Gaussian pulse train as

$$x_h(n) = \sum_i a \cdot exp(-(nT_s - 1/f_h)^2/2g^2), \quad (14)$$

where f_h is heartbeat frequency, a is the pulse amplitude, g is the width of the pulse, and T_s is sampling time. Fig. 9(a) is the arc of (14), in which the data points constituting the arc are non-uniformly distributed. In this distribution, the estimation performance is shown as solid lines in Fig. 9(b); the performance for the uniformly distributed arc data points is shows as dashed lines. The non-uniformness does not degrade the performance of the circumcenter estimation method for all SNRs. We consider the time required for MATLAB to compute the dc-offset estimation algorithm by using the profile function in MATLAB. For various SNRs, the execution times are shown in Table I, in which each time value refers to one execution time. The circumcenter method has the computation time of around 0.16 ms, which is not affected by SNR.

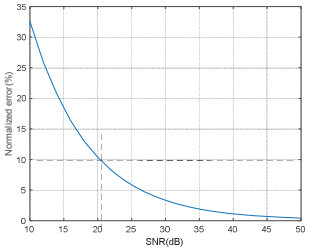

Fig. 8. The effect of *SNR* on the estimation performance

TABLE I
COMPUTATIONAL COMPLEXITY

SNR	Circumcenter/ms
10	0.165
20	0.165
30	0.16
40	0.16
50	0.16

Execution times are measured with 100 iterations and averaged for each simulation.

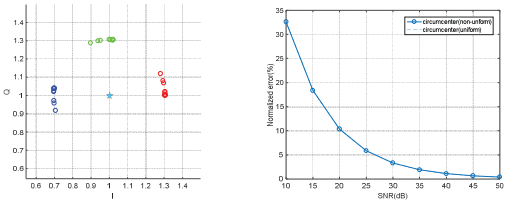

(a) (b)

Fig. 9. Non-uniform distribution of heartbeat data points and its performance: (a) the arc of (24) and (b) performance comparison of uniform and non-uniform distribution

V. CONCLUSIONS

Micro-Doppler radar is a promising technique for non-contact physiological signal sensing, such as sleep monitoring, driver drowsiness/fatigue detection, buried survivor searching, and other human motion classifying applications. The multi-frequency quadrature radar is useful for estimating the center of a circle where multiple arcs are placed by small movements, where they have discontinuities, i.e., the arc interval, are determined by Δf and d. This arc length extension was shown to help improve the performance of the abovementioned center estimation methods despite the discontinuities. For a given movement and distance of a target, the performance of the center estimation methods can be evaluated for different values of parameters such as f_c, Δf, and M. Through a series of simulations, the multiple CW quadrature radar is found to outperform the quadrature CW radar if the parameters are properly designed. The multiple CW quadrature radar can serve as a dc-tracking method for many real-time applications

ISBN 978-90-827970-1-5 © EURASIP 2018

because it can be implemented simply by using voltage-controlled CW radar hardware.

ACKNOWLEDGMENT

This work was supported by Electronics and Telecommunications Research Institute (ETRI) grant funded by the Korea government (MSIT) (18ZH1600, Robust Contactless Wearable Radar Technology with Motion Artifact Removal for Easy-to-Wear Vital-sign Sensing Devices)

.

REFERENCES

[1] M. Zakrzewski, A. Vehkaoja, A. S. Joutsen, K. T. Palovuori, and J. J. Vanhala, "Noncontact respiration monitoring during sleep with microwave Doppler radar," IEEE Sensors J., vol. 15, no. 10, pp. 5683–5693, Oct. 2015.

[2] M. Kagawa, K. Ueki, H. Tojima, and T. Matsui, "Noncontact screening system with two microwave radars for the diagnosis of sleep apneahypopnea syndrome," in Proc. Conf. IEEE Eng. Med. Biol. Soc., Osaka, Japan, Jul. 2013, pp. 2052–2055

[3] M. Baboli, A. Singh, and B. Soll, "Good Night: Sleep Monitoring Using a Physiological Radar Monitoring System Integrated with a Polysomnography System," *IEEE Microw. Mag.*, vol. 16, pp.34–41, 2016.

[4] B. Park, O. Lubecke, and V. Lubecke, "Arctangent demodulation with dc offset compensation in quadrature Doppler radar receiver systems," *IEEE Trans. Microw. Theory Tech.*, vol. 55, no. 5, pp. 1073–1079, May 2007.

[5] M. Zakrzewski, H. Raittnen, and J. Vanhala, "Comparison of center estimation algorithms for heart and respiration monitoring with microwave Doppler radar", *IEEE Sens. J.*, 12(3), pp. 627-634, 2012.

[6] Y. Yan, C. Li, and J. Lin, "Effects of I/Q mismatch on measurement of periodic movement using a Doppler radar sensor," in IEEE Radio Wireless Symp., 2010, pp. 196–199.

[7] A. Bjorck, "Solving linear least squares problems by gram-schmidt orthogonalization.," *BIT Numer. Math.*, vol. 7, no. 1, pp. 1–21, Jan. 1967.

[8] B.-K. Park, A. Vergara, O. Boric-Lubecke, V. Lubecke, and A. HøstMadsen, "Quadrature demodulation with DC cancellation for a Doppler radar motion detector," unpublished. Available: http://wwwee.eng.hawaii.edu/~madsen/Anders_Host-Madsen/Publications_2.html

[9] M. Huang, J. J. Liu, W. Xu, C. Gu, C. Li, and M. Sarrafzadeh, "A self-calibrating radar sensor system for measuring vital signs," *IEEE Trans. Biom. Cir. and Sys.*, 10, pp. 352–363, 2016.

[10] B. K. Park, S. Yamada, and V. M. Lubecke, "Measurement method for imbalance factors in direct-conversion quadrature radar systems," IEEE Microw. Wireless Compon. Lett., vol. 17, no. 5, pp. 403–405, May 2007.

[11] M. Zakrzewski, et al., "Quadrature Imbalance Compensation with Ellipse-Fitting Methods for Microwave Radar Physiological Sensing," *IEEE Trans. Microw. Theory Tech.*, vol.62, pp.1400–1408, 2013.

[12] E. Yavari, O. Boric-Lubecke., "Channel imbalance effects and compensation for doppler radar physiological measurements," IEEE Trans. Microw. Theory Tech., vol. 63, pp.3834-384, 2015.

[13] X. Gao, and O. Boric-Lubecke, "Radius Correction Technique for Doppler Radar Noncontact Periodic Displacement Measurement," *IEEE Trans. Microw. Theory Tech.*, vol. 65, pp. 621-631, Feb. 2018.

[14] W. Xu, C. Gu, C. Li, and M. Sarrafzadeh, "Robust Doppler radar demodulation via compressed sensing," *Electron. Lett.*, vol. 48, no. 22, pp. 1428–1430, Oct. 2012.

[15] H. Zhao, et al., "Accurate DC offset calibration of Doppler radar via non-convex optimization," *Electron. Lett.*, vol.51, pp.1282–1284, 2015.

[16] M. Jankiraman, B. Wessels, P. van Genderen, "PANDORA Multi frequency FMCW/SFCW Radar", 2000, Proc. Of the IEEE 2000 Int. Radar Conf., pp 750-757.

[17] A.W.Rihaczek, "Principles of high resolution radar", New York, McGrawHill, 1969; Los Altos, CA Peninsula Publishing, 1985;

[18] Free-space path loss, Wikipedia. Available: https://en.wikipedia.org/wiki/Free-space_path_loss.

[19] Circumcenter, WolframMathWorld. Available: http://mathworld.wolfram.com/Circumcenter.html.

[20] J. Wang, X. Wang, Z. Zhu, J. Huangfu, C. Li, and L. Ran, "1-D microwave imaging of human cardiac motion: An ab-initio investigation," *IEEE Trans. Microw. Theory Tech.*, vol. 61, no. 5, pp. 2101–2107, May 2013.

[21] M. Nosrati, and N. Tavassolian, "High-Accuracy Heart Rate Variability Monitoring Using Doppler Radar Based on Gaussian Pulse Train Modeling and FTPR Algorithm," *IEEE Trans. Microw. Theory Tech.*, vol. 66, pp. 556-567, Feb. 2018.

[22] D. Morgan, and M. Zierdt, "Novel signal processing techniques for Doppler radar cardiopulmonary sensing," Signal Processing, vol. 89, issue 1, Jan. 2009.

.